Optical bistability and nonlinear dynamics by saturation of cold Yb atoms in a cavity

Hannes Gothe,[1,2] Tristan Valenzuela,[2] Matteo Cristiani,[2] and Jürgen Eschner[1,2]
[1]*Experimentalphysik, Universität des Saarlandes, D-66123 Saarbrücken, Germany*
[2]*ICFO–The Institute of Photonic Sciences, Mediterranean Technology Park, Avenue Carl Friedrich Gauss 3, E-08860 Castelldefels (Barcelona), Spain*

(Received 10 August 2018; published 28 January 2019)

We observe optical bistability as well as oscillations in the upper bistable branch when cold ytterbium atoms are dispersively coupled to a high finesse optical cavity. Comparable previous observations were explained by atomic density oscillations in case of a Bose-Einstein condensate or optical pumping in case of a cold cloud of cesium. Both explanations do not apply in our case of thermal atoms with only a single ground state. We propose a simple two-level model including saturation to describe our experimental results. This paper introduces the experimental setup, derives the mentioned model, and compares it to our experimental data. Good quantitative agreement supports our model.

DOI: 10.1103/PhysRevA.99.013849

I. INTRODUCTION

Bistability describes a hysteresislike phenomenon where a system exposed to the same input values can reach two different states depending on its own history. In optics this typically occurs when a feedback-providing cavity is combined with a nonlinear medium. The nonlinearity might be either absorptive as for saturable absorbers or dispersive as for media that change their refractive index with light intensity. Many different materials like atomic vapors, ruby, Kerr liquids, and semiconductors were used and investigated starting in the 1970s [1,2], mainly driven by the search for all-optical logic and switching devices. Nowadays, also quantum systems like ultracold atoms, Bose-Einstein condensates (BEC), and superconducting qubits [3,4] are used as media while at the same time single photons became sufficient to produce bistable behavior [5,6], extending the scope of application from all-optical to quantum logic devices.

Here, we report the observation of optical bistability and oscillations in cold ytterbium extending similar studies with cold atoms [5,7] and with a BEC [6,8]. While the previous observations were explained by a competition of optical pumping and saturation [7] or atomic density oscillations [6], these explanations do not apply in our case: We study a thermal cloud instead of a BEC, and our atoms have only a single ground state, which thus excludes optical pumping processes. Therefore, we present a simple two-level model incorporating saturation that describes our observations. Our observations and their modeling add some new aspects to the existing results on optical bistability, in particular since oscillations on the upper bistable branch have so far not been reported for cold thermal atoms.

The paper starts by introducing our setup and measurement procedure in Sec. II. Section III derives a theoretical model, describes the principle working mechanism in Fig. 3, and compares the model quantitatively to our measurements of the steady-state behavior. Finally, Sec. IV discusses oscillations that occur in the upper bistable branch.

II. EXPERIMENT

Our setup (Fig. 1) consists of a cloud of cold ytterbium (^{174}Yb) atoms that are continuously trapped inside a high-finesse optical cavity. The magneto-optical trap (MOT) operates on the $^1S_0 \leftrightarrow {}^1P_1$ transition (see Table I) with an intensity of $\sim 0.5\, I_{\mathrm{sat}}$, a detuning of $0.86\,\Gamma$, and a magnetic field gradient of 36 G/cm. We trap about 10^7 atoms at a temperature of 3 mK [9]. The trap is constantly replenished by a Zeeman-slowed atomic beam from an atomic oven; the number of trapped atoms is adjusted by a mechanical shutter that controls the influx of new atoms.

Our cavity consists of two highly reflective mirrors in Fabry-Perot configuration. It is resonant with the $^1S_0 \leftrightarrow {}^3P_1$ transition (see Table I) and has a linewidth of $\kappa = 2\pi \times 70$ kHz (finesse $\mathcal{F} = 55\,000$) and a waist radius of $w_0 = 90\,\mu$m. We use a comparatively large cavity of 4.74 cm which leaves enough space to trap atoms directly inside the cavity [10]. This long cavity leads to an atom-photon coupling of $g_0 = 2\pi \times 30$ kHz corresponding to a cooperativity of $C = 0.1$ which is below the strong-coupling threshold for single atoms. Nevertheless, for a sufficient number of atoms ($N > 10$) we reach the collective strong coupling regime. We control and check the atom-cavity overlap by looking along the cavity axis using a CCD camera; the cavity mirrors are 90% transparent for blue light. Therefore, we observe the cavity mode and the trap stray light at the same time (Fig. 1), and by centering the MOT ($\approx$1-mm diameter) in the cavity we establish an overlap of $\lesssim$1% between all trapped atoms and the cavity mode. Thus, a typical number of $N \simeq 10^5$ atoms is coupled to the cavity.

For the measurements presented in this paper we pump the fundamental mode of the cavity with a pump frequency ω_{p} and a pump-cavity detuning $\Delta_{\mathrm{pc}} = \omega_{\mathrm{p}} - \omega_{\mathrm{c}}$ while we fix the cavity resonance ω_{c} at a detuning of $\Delta_{\mathrm{ca}} = \omega_{\mathrm{c}} - \omega_{\mathrm{a}} = +30$ MHz ($160\,\Gamma$) from the atomic resonance ω_{a} which makes the atoms a dispersive, rather than absorptive, medium inside the cavity. We then modulate the pump frequency in the vicinity of the

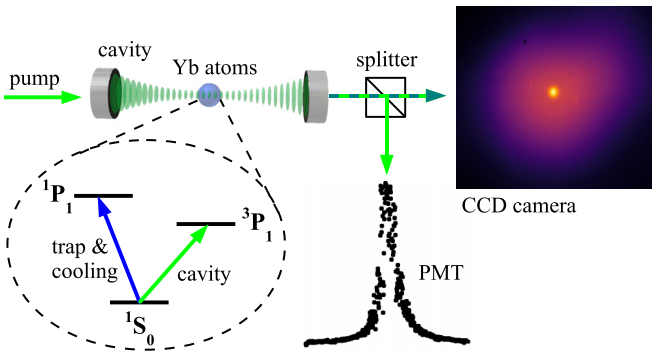

FIG. 1. Setup. We pump a high-finesse optical cavity and scan over its resonance recording the transmission curve with a photomultiplier tube (PMT). We trap cold ytterbium atoms inside the resonator using the strong, blue ${}^1S_0 \leftrightarrow {}^1P_1$ transition and tune the cavity field close to the narrow green ${}^1S_0 \leftrightarrow {}^3P_1$ transition. This induces strong dispersive effects between atoms and cavity field and leads to a deformation of the transmission peak. With a camera we monitor the spatial overlap of the atoms (large cloud) with the cavity mode (center dot).

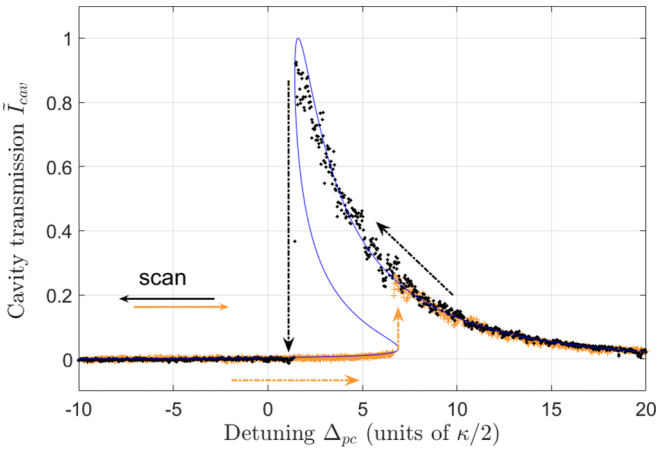

FIG. 2. The cavity transmission is measured in the presence of $\simeq$150 000 atoms by keeping the cavity fixed while changing the pump laser frequency. When scanning in positive direction we record the orange (gray) trace, whereas in negative direction we see the black one. We observe a bistable region ($\Delta_{pc} = 1 \ldots 7\,\kappa/2$) where two transmission values are possible depending on the scan direction. The blue (continuous) line depicts our model (5) with the parameters $A = 16$ and $S = 9$.

cavity resonance scanning over 1.234 MHz during 0.2 s at a pump power of 135 μW. We scan with both increasing and decreasing pump frequency and record the transmission with a photomultiplier tube (PMT). For calibration each scan is performed twice: once with an empty cavity and a second time with atoms. The center of the Lorentzian peak in the absence of atoms defines zero pump detuning. The presence of atoms inside the cavity alters the transmission profile significantly, showing typical signatures of optical bistability. For low atom numbers the Lorentzian curve becomes asymmetric and for higher atom numbers we record steep rises and drops at different frequencies depending on the scan direction (Fig. 2).

III. MODEL

In this section we develop a model that describes how the cavity transmission line shape is modified by the presence of atoms. Such a model has already been presented for a BEC and low photon numbers [6] and has been elaborated further into the quantum regime [8,11–14]. In our setup, in contrast, we have a thermal cloud and a mean intracavity photon number much higher than one. Therefore, our model is formulated in a classical framework. Importantly, it adds saturation effects at higher intracavity intensities. A related treatment was previously introduced by Lambrecht *et al.* [7] for the case of cold cesium atoms, where optical pumping plays an essential role and leads to pulsing in the bistable region. Here, we model our case of two-level atoms, i.e., without optical pumping, and study different phenomena, in particular oscillations around the steady state that appear inside and outside the bistability regime.

TABLE I. Characteristics of the used ytterbium transitions.

Transition	Wavelength λ(nm)	Linewidth $\Gamma/2\pi$ (MHz)	Saturation intensity I_{sat} (mW/cm^2)
${}^1S_0 \leftrightarrow {}^1P_1$	398.9	29	59
${}^1S_0 \leftrightarrow {}^3P_1$	555.8	0.182	0.14

The interplay of intracavity light field and atomic two-level population difference that the model describes is qualitatively explained in Fig. 3. The reminder of this section discusses the steady-state solution of the model while Sec. IV describes the dynamics of the system, appearing as oscillations around the steady state.

In an empty cavity that is pumped by a laser beam with frequency ω_p and an electric field amplitude E_{in}, the intracavity field E_{cav} evolves according to

$$\frac{d}{dt}E_{cav}(t) = i\frac{\kappa}{2}\sqrt{G}E_{in} - \frac{\kappa}{2}E_{cav}(t) + i\Delta_{pc}E_{cav}(t), \qquad (1)$$

where κ is the cavity linewidth (FWHM), $\Delta_{pc} = \omega_p - \omega_c$ the detuning between the pump and the cavity resonance frequency, $G = T/(1-R)^2$ the power enhancement factor, and T and R the transmittance and reflectivity of the cavity mirrors. The steady-state solution of (1) is

$$|E_{cav}|^2 = G|E_{in}|^2\frac{\kappa^2}{\kappa^2 + 4\Delta_{pc}^2}. \qquad (2)$$

This is a Lorentzian-shaped resonance curve, which is typical for an empty cavity.

Atoms inside the cavity act as an optical medium and therefore increase the optical cavity length and shift the cavity resonance. This leads to an effective detuning,

$$\Delta_n = \frac{g_0^2}{6\Delta_{ca}}N_\delta, \qquad (3)$$

which adds to Δ_{pc} in (2). It is proportional to the population difference $N_\delta = N_S - N_P$ between ground and excited state and to the shift due to a single maximally coupled

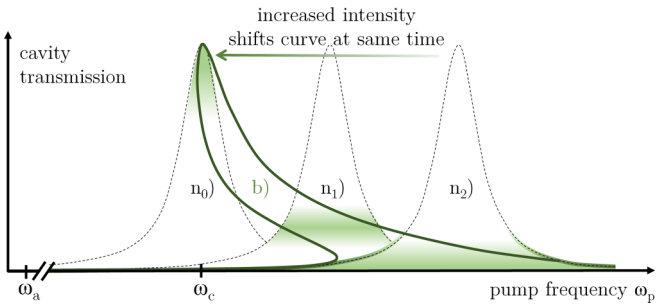

FIG. 3. The working principle of dispersive bistability: An empty cavity shows a Lorentzian-shaped resonance curve (n_0) when a pump laser is scanned across the cavity resonance frequency (ω_c). Atoms inside the cavity act as a dispersive medium and shift the resonance curve depending on their number (n_1, n_2). In turn, the effective atom number depends on the intracavity light intensity. With increasing intensity, more and more atoms get pumped to the excited state; they become transparent to the pump light and do not cause a dissipative shift anymore. This mutual influence between intracavity light intensity and effective atom number alters the shape of the resonance curve. When the cavity is filled with atoms and its resonance (n_2) is approached, the light intensity increases, bleaches a part of the atoms, and therefore shifts the resonance frequency towards ω_c (empty cavity). Each intensity level corresponds to a different position of the resonance curve as indicated by the green (shaded) areas. For low intensities the resonance frequency shifts linearly with the intensity ($n_2 \rightarrow n_1$) causing the resulting resonance curve (b) to be tilted. For higher intensities ($I \gtrsim I_{sat}$) the optical pumping saturates as most of the atoms are already bleached, and the resonance shift reduces ($n_1 \rightarrow n_0$) and the resulting curve (b) bends upwards at its tip.

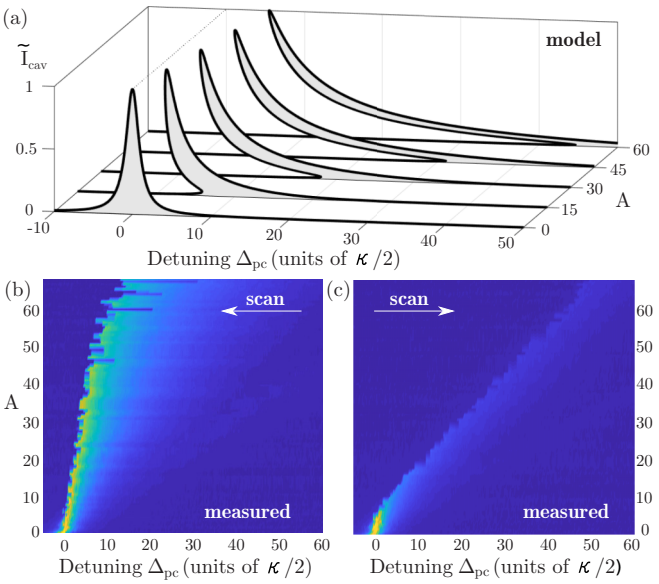

FIG. 4. Comparison of our model and the measured data for different atom numbers. The upper plot (a) shows calculations of the normalized cavity transmission $\tilde{I}_{cav}$ according to (5) for different detunings $\tilde{\Delta}_{pc}$ and atom-cavity interaction strength ($A = 0 \ldots 60$), where A is proportional to the atom number. The parameter S is set to 8. This yields a Lorentzian curve for no atoms and increasingly tilted curves for larger atom numbers. The lower plots show a corresponding set of experimental data with frequency scans across the cavity resonance in negative (b) and positive (c) scan direction. Each horizontal line represents one frequency scan at a fixed atom number (see Fig. 2). The obtained transmission is color coded, blue representing low intensity and red high intensity. The atom number, indicated by parameter A, is varied along the vertical axis.

atom, g_0^2/Δ_{ca}, where g_0 is the atom cavity coupling rate and $\Delta_{ca} = \omega_c - \omega_a$ the cavity atom detuning. Corresponding to the experiment, we assume that $\Delta_{ca} \gg \Gamma$. A factor $\frac{1}{3}$ arises from averaging over the three possible directions of atomic orientation. Another factor $\frac{1}{2}$ comes from an intensity average along the standing wave of the cavity. If all atoms are in the ground state ($N_S = N = N_\delta$) they all contribute to the resonance shift. In contrast, if the transition is saturated ($N_\delta = 0$) the atoms are transparent to this light. For two-level atoms N_δ is given by

$$N_\delta = N\left(1 + \frac{\Gamma^2|E_{cav}|^2}{4\Delta_{ca}^2 I_{sat}}\right)^{-1}. \tag{4}$$

The factor $4\Delta_{pa}^2/\Gamma^2$ in front of the on-resonance saturation intensity I_{sat} accounts for the pump detuning with respect to the atomic resonance. Here we assume that $\Delta_{pa} = \Delta_{pc} + \Delta_{ca} \simeq \Delta_{ca}$ since the pump-cavity detuning Δ_{pc} is small compared to Δ_{pa} and Δ_{ca}.

Inserting (4) into (3) and adding (3) to Δ_{pc} in (2) gives

$$|E_{cav}|^2 = G|E_{in}|^2 \frac{\kappa^2}{\kappa^2 + 4\left[\Delta_{pc} + \frac{Ng_0^2}{6\Delta_{ca}}\left(1 + \frac{\Gamma^2|E_{cav}|^2}{4\Delta_{ca}^2 I_{sat}}\right)^{-1}\right]^2}.$$

We introduce a normalized detuning $\tilde{\Delta}_{pc} = 2\Delta_{pc}/\kappa$, an intracavity intensity $\tilde{I}_{cav} = |E_{cav}/E_{in}|^2/G$ that is normalized to its maximum value at resonance, and two constants A and S leading to

$$\tilde{I}_{cav} = \frac{1}{1 + [\tilde{\Delta}_{pc} + A(1 + S\tilde{I}_{cav})^{-1}]^2}. \tag{5}$$

The constant,

$$A = \frac{Ng_0^2}{3\Delta_{ca}\kappa}, \tag{6}$$

expresses the atom-cavity interaction strength, and the saturation parameter,

$$S = \frac{GI_{in}\Gamma^2}{4\Delta_{ca}^2 I_{sat}}, \tag{7}$$

is the ratio between the on-resonance intracavity intensity and the detuned saturation intensity. In our experiments, A and S are determined by the atom number N and the input intensity I_{in}, respectively. The parameters of Fig. 2 ($N \simeq 150\,000$, $I_{in} = 135\,\mu$W) correspond to $A \simeq 20$ and $S \simeq 12$. A fit results in $A = 16$ and $S = 9$. Taking into account the uncertainties especially for estimating the atom number from the MOT stray light we consider this a satisfactory agreement.

The parameters A and S define the shape of the resonance curve. The influence of A is illustrated in Fig. 4. For $A = 0$ the resonance curve is symmetric and centered at zero detuning. For larger values the curve becomes increasingly

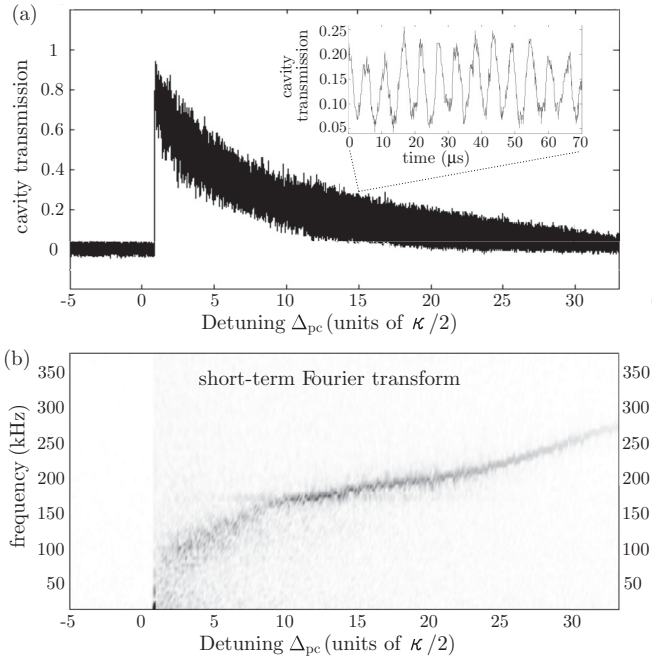

FIG. 5. (a) Oscillation of the cavity transmission during a scan with decreasing detuning. The scan was performed in 68 ms with 250 000 atoms overlapped to the cavity mode. The inset shows a zoom at $\tilde{\Delta}_{pc} = 15$ revealing oscillations on a μs time scale. (b) A short-term Fourier transform obtained from local sections of the transmission signal shows how the oscillation frequency is changing during the scan.

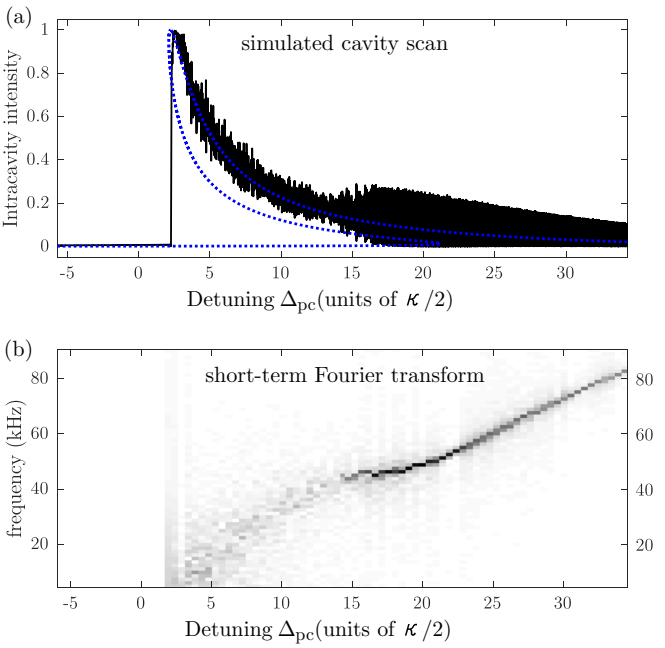

FIG. 6. (a) (Self-)oscillations appear when we numerically simulate a cavity scan with the parameters of the measurement in Fig. 5 (decreasing detuning, $N = 250\,000$, $A = 35$, $S = 15$, 68-ms scan time with 8-ns time step). The dotted blue line depicts the steady-state solution according to Eq. (5). (b) Time-dependent oscillation frequency obtained from a short-term Fourier transform of the simulated intracavity intensity. It reveals a qualitatively similar change of the oscillation frequency as in Fig. 5(b); the simulated frequencies, however, are about four times lower than the observed ones.

shifted and tilted. For sufficiently high atom number it exhibits a bistable region with multiple solutions. This leads to a hysteresis effect, whereby one branch of solutions is followed when entering the bistable region from one side but another branch when entering from the opposite side. In Figs. 4(b) and 4(c) the high- and the low-intensity branch is experimentally observed when scanning in negative or positive direction, respectively.

IV. OSCILLATIONS

Many of our scans show oscillations of the cavity transmission on a μs time scale. The previous plots (Fig. 2) were averaged to remove these fast oscillations. Now we will focus on them.

The oscillations occur in both scanning directions throughout all the transmission region. They are most evident in the upper bistable branch when scanning with decreasing detuning and using many atoms (250 000), as depicted in the example of Fig. 5. Even higher atom numbers tend to collapse the upper branch as the system gets unstable and abruptly settles to the lower branch. The frequency of the oscillation changes between 100 and 300 kHz while scanning [see Fig. 5(b)]. When less atoms are used, the tail of the whole resonance shortens but the oscillation frequency at a certain detuning stays the same. Interestingly, the frequency is close to the atomic decay rate of 182 kHz even though a change of the transmission properties should be limited by the cavity decay (70 kHz).

For comparison with the model we numerically simulate a scan with the parameters from the experiment (Fig. 5), using

$$\frac{d}{dt}N_\delta = \Gamma N - \Gamma N_\delta\left(1 + \frac{I_{cav}}{I_{sat}}\right), \tag{8}$$

for the evolution of the population difference, and using Eq. (1) for the evolution of the intracavity field, where we include the dispersive shift of Eq. (3) into Δ_{pc}. We also take the absorptive effects of the atoms inside the cavity into account, by using an effective cavity decay rate,

$$\kappa_{eff} = \kappa + \epsilon_a N_\delta / T, \tag{9}$$

where T is the cavity round-trip time, and

$$\epsilon_a = \frac{1}{3}\frac{\lambda^2}{\pi w_0^2/4}\frac{\Gamma^2}{4\Delta_{ca}^2} = 6 \times 10^{-10} \tag{10}$$

estimates the round-trip loss per atom in the cavity. The individual factors in ϵ_a account for the polarization matching, the atomic scattering cross section within the cavity mode, and the detuning.

As displayed in Fig. 6(a), the simulation yields kHz oscillations that change their frequencies during the scan [Fig. 6(b)] in a similar way as the ones observed experimentally. One notes, however, that the calculated frequencies are about four

times smaller than the measured ones. A similar discrepancy was found in [6] and will need further investigation.

Moreover, the result of the simulation shows a division into a region of stable, self-sustained oscillations for $\tilde{\Delta}_{\mathrm{pc}} > 15$, and a region of unsteady oscillations for $\tilde{\Delta}_{\mathrm{pc}} < 15$. Closer inspection reveals that the oscillations are undamped in the stable regime, whereas they are damped in the unstable regime. Such a division may also be identified in the experimental traces, such as in Fig. 5 around $\tilde{\Delta}_{\mathrm{pc}} \simeq 12$, although the observed oscillations continue rather smoothly across the regimes. We attribute this to unavoidable fluctuations in the experiment that continually trigger new oscillations also in the damped regime. To account for this in the simulations, we added a small noise contribution to the atom number (normally distributed with $\sigma = 0.012N$ and added to N_δ in each time step). This noise excites the oscillations displayed in Fig. 6 for $\tilde{\Delta}_{\mathrm{pc}} \leqslant 15$. The amplitude of the noise was not based on an estimate from the experiment but chosen such that the two regions of lower and higher damping are distinguishable. With more noise the regions merge seamlessly, which may explain why they are not distinguished in Fig. 5. The origin and the mathematical background of the differently damped oscillations could not yet be fully clarified and will also be the subject of further investigations.

V. DISCUSSION

We observe bistability of the intracavity power when a high-finesse cavity containing a large number of thermal atoms (mK regime) is near-resonantly excited through a mirror. Our observations are phenomenologically similar to the ones previously reported for a BEC [6] and for cold cesium [7], but they are obtained in a different physical system and hence suggest that a different mechanism of nonlinear atom-light interaction must be at work. In the optomechanical model for the BEC system, the coupling decreases when atoms move from an antinode to a node of the cavity lattice, while for cold cesium it increases when the atoms are pumped to higher Zeeman states. In our model, in contrast, the atom-cavity coupling diminishes when part of the atoms are pumped to the excited state. Nevertheless, all mechanisms lead to mathematically similar equations and similar phenomena. Interestingly, our model also predicts oscillations around the bistable solutions of the nonlinear equations, but the calculated oscillation frequencies deviate from the observed ones by about a factor of 4, similar to the result in [6]. Furthermore, the simulations suggest that there are regimes of undamped and of damped oscillations, whose origins will require further mathematical investigation.

ACKNOWLEDGMENTS

The authors acknowledge discussions with O. Mishina. This work was partially supported by the Deutsche Forschungsgemeinschaft (D-A-CH "Quantum crystals of matter and light", ES339/1-1).

[1] A. Szöke, V. Daneu, J. Goldhar, and N. A. Kurnit, Appl. Phys. Lett. **15**, 376 (1969).
[2] H. M. Gibbs, *Optical Bistability: Controlling Light with Light* (Academic Press, Cambridge, 1985).
[3] H. Ritsch, P. Domokos, F. Brennecke, and T. Esslinger, Rev. Mod. Phys. **85**, 553 (2013).
[4] A. Blais, R.-S. Huang, A. Wallraff, S. M. Girvin, and R. J. Schoelkopf, Phys. Rev. A **69**, 062320 (2004).
[5] S. Gupta, K. L. Moore, K. W. Murch, and D. M. Stamper-Kurn, Phys. Rev. Lett. **99**, 213601 (2007).
[6] S. Ritter, F. Brennecke, K. Baumann, T. Donner, C. Guerlin, and T. Esslinger, Appl. Phys. B **95**, 213 (2009).
[7] A. Lambrecht, E. Giacobino, and J. Courty, Opt. Commun. **115**, 199 (1995).
[8] F. Brennecke, S. Ritter, T. Donner, and T. Esslinger, Science **322**, 235 (2008).
[9] M. Cristiani, T. Valenzuela, H. Gothe, and J. Eschner, Phys. Rev. A **81**, 063416 (2010).
[10] Typical setups [15–17] use short cavities of $\simeq$100 μm in order to reach the strong coupling regime; the atoms are externally prepared and then moved into the cavity.
[11] D. Nagy, P. Domokos, A. Vukics, and H. Ritsch, Eur. Phys. J. D **55**, 659 (2009).
[12] B. Prasanna Venkatesh, M. Trupke, E. A. Hinds, and D. H. J. O'Dell, Phys. Rev. A **80**, 063834 (2009).
[13] M. Diver, G. R. M. Robb, and G.-L. Oppo, Phys. Rev. A **89**, 033602 (2014).
[14] B. P. Venkatesh and D. H. J. O'Dell, Phys. Rev. A **88**, 013848 (2013).
[15] T. P. Purdy, D. W. C. Brooks, T. Botter, N. Brahms, Z.-Y. Ma, and D. M. Stamper-Kurn, Phys. Rev. Lett. **105**, 133602 (2010).
[16] P. Münstermann, T. Fischer, P. W. H. Pinkse, and G. Rempe, Opt. Commun. **159**, 63 (1999).
[17] H. Mabuchi, J. Ye, and H. J. Kimble, Appl. Phys. B **68**, 1095 (1999).